Int. J. Electrochem. Sci., 9 **(2014)** 5479 - 5495

International Journal of
ELECTROCHEMICAL
SCIENCE
www.electrochemsci.org

Corrosion Inhibition of Steel in HCl by 2-Aminoethyl diphenylborinate

L. Afia[1], *R. Salghi*[1,*], *Eno. E. Ebenso*[2,*], *M. Messali*[3], *S. S. Al-Deyab*[4], *B. Hammouti*[5]

[1] Laboratory of Environmental Engineering and Biotechnology, ENSA, Université Ibn Zohr, PO Box 1136, 80000 Agadir, Morocco
[2]Material Science Innovation & Modelling (MaSIM) Research Focus Area, Faculty of Agriculture, Science and Technology, North-West University (Mafikeng Campus), Private Bag X2046, Mmabatho 2735, South Africa
[3] Chemistry Department, Faculty of Science, Taibah University, 30002, Al-Madinah Al-Mounawwara, Saudi Arabia.
[4] Petrochemical Research Chair, Chemistry Department, College of Science, King Saud University, P.O. Box 2455, Riyadh 11451, Saudi Arabia
[5]LCAE-URAC18, Faculté des Sciences, Université Mohammed Premier, B.P. 4808, 60046, Oujda, Morocco
[*]E-mail: r.salghi@uiz.ac.ma; Eno.Ebenso@nwu.ac.za

Received: 14 April 2014 / *Accepted:* 19 June 2014 / *Published:* 16 July 2014

The corrosion behavior of C38 steel in HCl solution with different concentration of 2-Aminoethyl diphenylborinate $C_{14}H_{16}BNO$(DDB) was investigated by weight loss and electrochemical measurements. Results obtained reveal that DDB performs excellently as corrosion inhibitor for C38 steel in 1.0 M HCl. Potentiodynamic polarization studies have shown that DDB behaves as mixed-type inhibitors. Also, the inhibition efficiency was found to increase with increase of the inhibitor concentrations to reach 97.8 % at 2.10^{-3} M of DDB due to the adsorption of the inhibitor molecules on the metal surface and the adsorption follows Langmuir's adsorption isotherm. EIS spectra exhibit one capacitive loop and confirm the inhibitive ability. Double layer capacitance and charge transfer resistance values were derived from Nyquist plots obtained from impedance studies. Data obtained from EIS measurements, were analyzed to model the corrosion inhibition process through appropriate equivalent circuit model; a constant phase element (CPE) has been used.

Keywords: Corrosion, Steel, Inhibition, DDB, Acid solution.

1. INTRODUCTION

Corrosion is a fundamental process playing an important role in economics and safety, particularly for metals and alloys. Steel has found wide applications in a broad spectrum of industries and machinery;

despite its tendency to corrosion. Because of the aggressiveness of acid solutions, inhibitors are commonly used to reduce the corrosive attack on metallic materials. Organic compounds rich in heteroatoms such sulphur, nitrogen and oxygen generally exhibit the best protection among corrosion [1–29]. The inhibitor adsorption mode was strictly dependent on the inhibitor structure [30]. Data in the literature show that most organic inhibitors adsorb on metals by displacing water molecules on the surface and forming a compact barrier film [30–32]. Adsorption of inhibitors may blocks either cathodic, anodic, or both reactions.

The synthesis of new organic molecules offers various molecular structures containing several heteroatoms and substituents. In continuation of the encouraging results obtained by different synthetic inhibitors, we investigate the corrosion of C38 steel in 1 M HCl by DDB compound, Scheme 1. Weight loss tests and electrochemical techniques (potentiodynamic polarisation and impedance measurements) have been used to study the effect of addition of this compound on the corrosion of steel in hydrochloric acid solution (1 M HCl) in the 298–328 K range.

2. MATERIALS AND METHODS

2.1. Synthesis of the DDB

The organic compound 2-Aminoethyl diphenylborinate (*DDB*) was obtained from Germany Chemical Reagent Company. Fig. 1 shows the molecular structure of *DDB.*

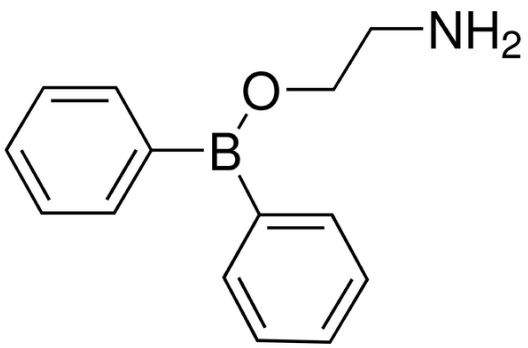

Figure 1. shows the molecular formula of the investigated compound.

2.2. Electrochemical tests

The electrochemical study was carried out using a potentiostat PGZ100 piloted by Voltamaster software. This potentiostat is connected to a cell with three electrode thermostats with double wall (Tacussel Standard CEC/TH). A saturated calomel electrode (SCE) and platinum electrode were used as reference and auxiliary electrodes, respectively. The material used for constructing the working electrode was the same used for gravimetric measurements. The surface area exposed to the electrolyte is 0.056 cm^2. Potentiodynamic polarization curves were plotted at a polarization scan rate of 0.5 mV/s. Before all experiments, the potential was stabilized at free potential during 30 min. The polarisation curves are obtained from −700 mV to −300 mV at 298

K. The solution test is there after de-aerated by bubbling nitrogen. Gas bubbling is maintained prior and through the experiments. In order to investigate the effects of temperature and immersion time on the inhibitor performance, some test were carried out in a temperature range 298–328 K. The electrochemical impedance spectroscopy (EIS) measurements are carried out with the electrochemical system (Tacussel), which included a digital potentiostat model Voltalab PGZ100 computer at E_{corr} after immersion in solution without bubbling. After the determination of steady-state current at a corrosion potential, sine wave voltage (10 mV) peak to peak, at frequencies between 100 kHz and 10 mHz are superimposed on the rest potential. Computer programs automatically controlled the measurements performed at rest potentials after 0.5 hour of exposure at 298 K. The impedance diagrams are given in the Nyquist representation. Experiments are repeated three times to ensure the reproducibility.

2.3. Weight loss measurements

Coupons were cut into 2 × 2 × 0.08 cm^3 dimensions having composition (0.179% C, 0.165% Si, 0.439% Mn, 0.203% Cu, 0.034% S and Fe balance) are used for weight loss measurements. Prior to all measurements, the exposed area was mechanically abraded with 180, 320, 800 grades of emery papers. The specimens are washed thoroughly with bidistilled water, degreased and dried with ethanol. Gravimetric measurements are carried out in a double walled glass cell equipped with a thermostated cooling condenser. The solution volume is 80 cm^3. The immersion time for the weight loss is 8 h at 298 K.

2.4. Solutions preparation

The aggressive solution (1M HCl) was prepared by dilution of analytical grade 37% HCl with double distilled water. The solution tests are freshly prepared before each experiment. Triplicate experiences were made to ensure the reproducibility.

3. RESULTS AND DISCUSSION

3.1. Effect of concentration

3.1.1. Polarization curves

Fig. 2 collects the potentiodynamic polarisation curves of steel in molar HCl in the presence and absence of different concentrations of DDB. The corresponding electrochemical parameters values of corrosion current densities (I_{corr}), corrosion potential (E_{corr}), cathodic Tafel slope (β_c), anodic Tafel slope (β_a) and inhibition efficiency (E_I %) for different concentrations of DDB are summarised in Table 1.

In this case, the inhibition efficiency is defined as follows:

$$E\% = (1 - \frac{I'_{corr}}{I_{corr}})x100 \quad (1)$$

Where I_{corr} and I'_{corr} are current density in absence and presence of DDB respectively. We noted that I_{corr} and I'_{corr} was calculated from the intersection of cathodic and anodic Tafel lines.

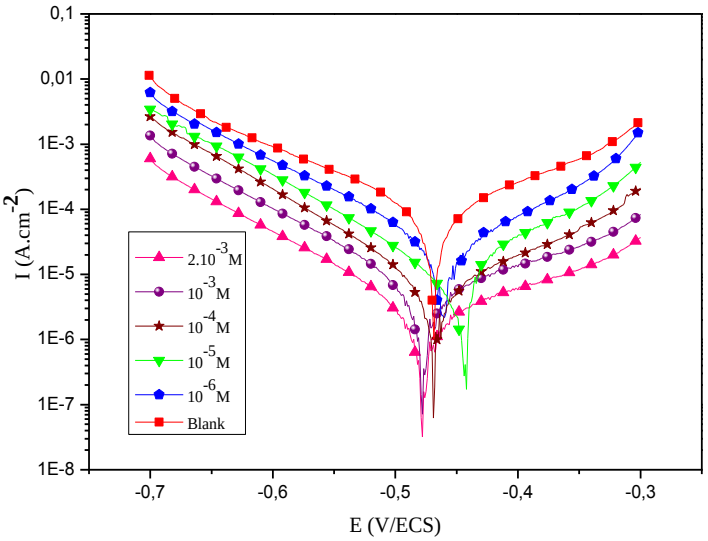

Figure 2. Polarisation curves for steel at various concentrations of DDB in molar HCl

Table 1. Electrochemical parameters of C38 steel at various concentrations of DDB in 1M HCl and corresponding inhibition efficiency.

Conc. (M)	E_{corr} (mV/SCE)	I_{corr} ($\mu A/cm^2$)	$-\beta_c$ (mV/dec)	β_a (mV/dec)	E_I (%)
Blank	- 467	94	99	108	-
10^{-6}	- 461	31	108	95	67.0
10^{-5}	- 443	11	96	92	88.3
10^{-4}	- 469	8	91	91	91.5
10^{-3}	- 478	7	99	106	92.6
2.10^{-3}	- 477	2.7	103	119	97.1

As it is schown in Fig.2, the cathodic current–potential curves give rise to parallel Tafel lines, which indicate that hydrogen evolution reaction is activation controlled and that the addition of the DDB does not modify the mechanism of this process [33]. Addition of DDB affects both anodic dissolution of steel and cathodic reduction reactions indicating that the compound could be classified as mixed-type inhibitors. The anodic and cathodic Tafel slopes (βa and βc) are approximately constant suggesting that the inhibiting action occurred by simple blocking of the available cathodic and anodic sites on the metal surface. We also remark that the polarization curves are shifted toward more negative potentials and less current density upon addition of DDB, this result can be explained by the

inhibitive action of DDB on cathodic branches. This result confirms the inhibitive action of the DDB toward acid corrosion of steel [34].

Table 1 shows that the values of I_{corr} decrease with the rise of DDB concentration. We note that the corrosion current densities were significantly reduced in the presence of DDB and became only 11 $\mu A/cm^2$ at 10^{-5} M. The higher efficiency obtained is 97.1% at 2.10^{-3} M of DDB.

3.1.2. Electrochemical impedance spectroscopy measurements

Fig. 3 shows the Nyquist plots for C38 steel in 1 M HCl solution in the absence and presence of different concentrations of the DDB at 298K.

The obtained Nyquist impedance diagrams in most cases does not show perfect semicircle, generally referred to the frequency dispersion of interfacial impedance. This anomalous phenomenon may be attributed to the inhomogeneity of the electrode surface arising from surface roughness or interfacial phenomena [35]. The data reveal that, each impedance diagram consists of a large capacitive loop with low frequencies dispersion (inductive arc). The shape is maintained throughout the whole concentrations, indicating that almost no change in the corrosion mechanism occurred due to the inhibitor addition [36].The electrochemical impedance parameters derived from these investigation are mentioned in Table 2.

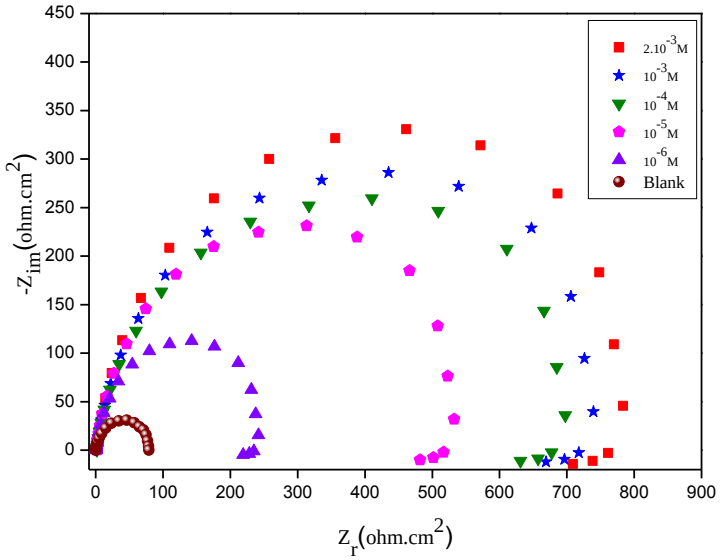

Figure 3. Nyquist diagrams for C38 steel electrode with and without DDB at E_{corr}

The inhibition efficiency can be calculated by the following formula:

$$E_{Rt}\% = \frac{(R_t - R^\circ_t)}{R_t} x100 \qquad (2)$$

Where R_t and R^0_t are the charge transfer resistances in inhibited and uninhibited solutions respectively.

The values of the polarization resistance were calculated by subtracting the high frequency intersection from the low frequency intersection [37]. Double layer capacitance values were obtained at maximum frequency (f_{max}), at which the imaginary component of the Nyquist plot is maximum, and calculated using the following equation:

$$C_{dl} = \frac{1}{2.\pi.f_m.R_t} \quad (3)$$

With C_{dl}: Double layer capacitance ($\mu F.cm^{-2}$); f_{max}: maximum frequency (Hz) and R_t: Charge transfer resistance ($\Omega.cm^2$).

Table 2. Electrochemical Impedance parameters for corrosion of steel in acid medium at various contents of DDB.

Conc. (M)	R_t ($\Omega.cm^2$)	f_{max}(Hz)	C_{dl}($\mu F/cm^2$)	E_{RT} (%)
Blank	74	79	27.24	-
10^{-6}	242	44	14.95	69.4
10^{-5}	532	38	7.88	86.1
10^{-4}	698	30	7.60	89.4
10^{-3}	740	22	9.78	90.0
2.10^{-3}	788	21	9.62	90.6

When a non-ideal frequency response is present, it is commonly accepted to employ distributed circuit elements in an equivalent circuit. The most widely used is the constant phase element (CPE), which has a non-integer power dependence on the frequency [38]. Often a CPE is used in a model in place of a capacitor to compensate for non-homogeneity in the system. The impedance of a CPE is described by the expression:

$$Z_{CPE} = Y^{-1}(j\omega)^{-n} \quad (4)$$

Where R_S is the solution resistance, R_{ct} is the charge transfer resistance and CPE is a constant phase element, Y is the magnitude of CPE, ω is the angular frequency ($2\pi f_{max}$), and the deviation parameter n is a valuable criterionof the nature of the metal surface and reflects microscopic fluctuations of the surface. For n = 0, Z_{CPE} representsresistance with $R = Y^{-1}$; n = -1 an inductance with $L = Y^{-1}$, n = 1 an ideal capacitor with C = Y [38].

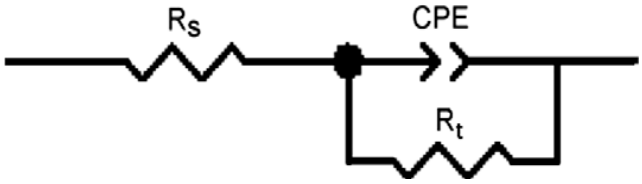

Figure 4. The electrochemical equivalent circuit used to fit the impedance spectra.

The idealized capacitance (C_{id}) values can be described by CPE parameter values Y and n using the following expression [49]:

$$C_{id} = Y\omega^{n-1}/\sin(n^{\pi/2}) \quad (5)$$

Fig. 4 shows the electrical equivalent circuit employed to analyze the impedance spectra with one capacitive loop [40, 41]. As an example, the Nyquist plots in 1M HCl solution in the absence and presence of 10^{-4} M of DDB are presented in Fig. 5 and 6 respectively.

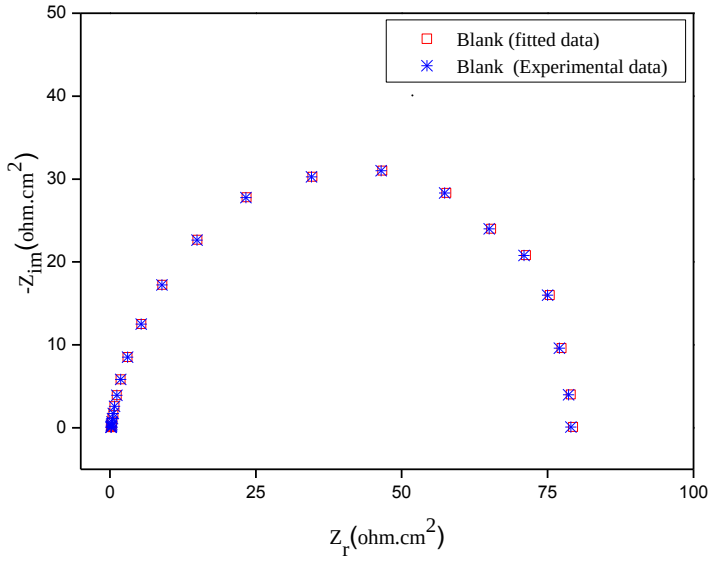

Figure 5. EIS Nyquist plots for mild steel in 1M HCl

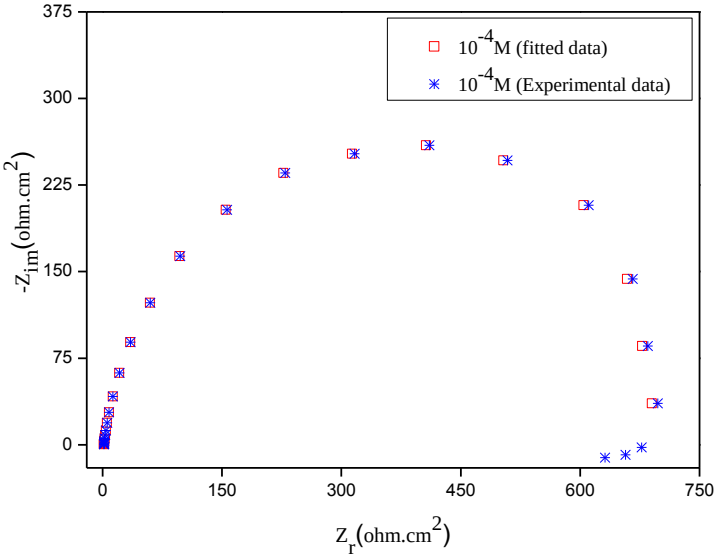

Figure 6. EIS Nyquist plots for mild steel in 1M HCl + 10^{-4} M of DDB interface.

Excellent fit with this model was obtained with our experimental data (Figs. 5 & 6). It is observed that the fitted data match the experimental, with an average error of about 0.01%. R_t values were

simultaneously determined by analysis of the complex-plane impedance plots and the equivalent circuit model and the result are very similar with insignificant changes. From the impedance data given in Table 2, we note that introduction of DDB into the acid solution caused the charge transfer resistance to increase, while reducing the double-layer capacitance. This effect becomes more pronounced at higher DDB concentration. This increase in the diameter of the Nyquist semicircle (R_t values), including the corresponding increase in the magnitude of the phase angle peaks in inhibited solutions, points toward improved corrosion resistance due to the corrosion-inhibiting action of DDB. The decrease in C_{dl} values, which normally results from a decrease in the dielectric constant and/or an increase in the double-layer thickness, can be attributed to the adsorption of this compound on the metal surface leading to the formation of a surface film in the acidic solution [42]. The efficiency increases with DDB concentration to reach 90.6% at 2.10^{-3}M. The results obtained from the electrochemical techniques in acidic solution were in good agreement with an insignificant variation.

3.1.3. Weight loss, corrosion rates and inhibition efficiency

The weight loss of C38 steel in 1M HCl in the absence and the presence of various concentrations of DDB was determined after 8 h of immersion period at 298K. Inhibition efficiency E_w (%) is calculated as follows:

$$E_W(\%) = \frac{W_{corr} - W'_{corr}}{W_{corr}} \times 100 \qquad (6)$$

Where W_{corr} and W'_{corr} are the corrosion rate of C38 steel in 1M HCl in absence and presence of inhibitor, respectively.

Table 3 regroups the results of weight loss of steel in 1M HCl with and without the addition of various concentrations of the DDB.

Table 3. Effect of DDB concentration on corrosion data of steel in 1M HCl

Conc. (M)	W'_{corr} (mg. cm^{-2})	E_w (%)
Blank	1.8614	-
10^{-6}	0.6207	66.7
10^{-5}	0.2196	88.2
10^{-4}	0.1617	91.3
10^{-3}	0.1268	93.2
2.10^{-3}	0.0402	97.8

Figs. 7 & 8 illustrate the variation of corrosion rate and efficiencies with concentration of inhibitor.

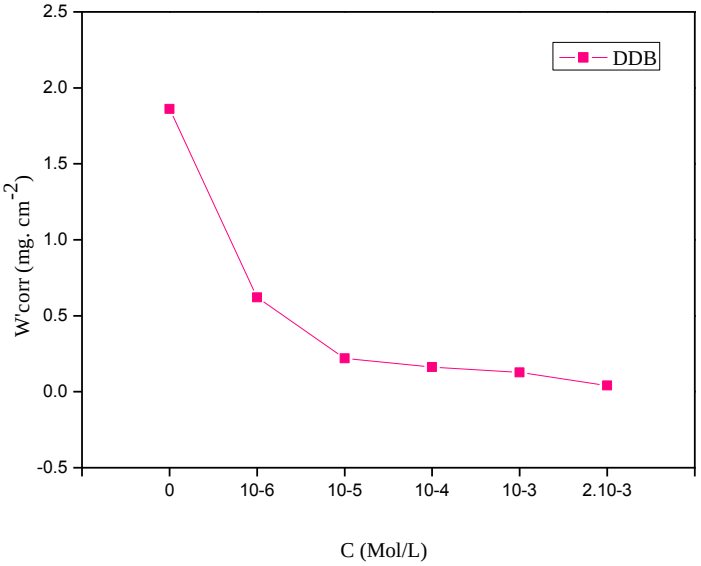

Figure 7. Variation of corrosion rate (W) with DDB compound concentration for steel in 1M HCl at 298 K

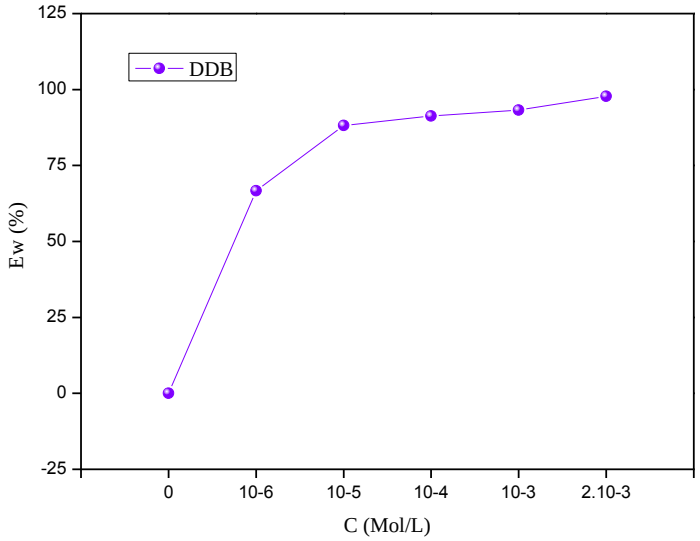

Figure 8. Variation of inhibition efficiency (E) with DDB compound concentration for steel in 1M HCl at 298 K

Results obtained from gravimetric measurements show that the steel corrosion rate values decrease when the concentration of DDB increases (Fig.7). The corrosion inhibition can be attributed to the adsorption of the DDB at the steel/acid solution interface. This result suggests that increase in inhibitor concentration increases the number of molecules adsorbed onto steel surface and reduces the surface area that is available for the direct acid attack on the metal surface. The highest inhibition efficiency 97.8% was obtained at 2.10^{-3}M of DDB.

The inhibition efficiencies, calculated from weight loss measurements, show the same trend as those obtained from electrochemical studies (Fig.9).

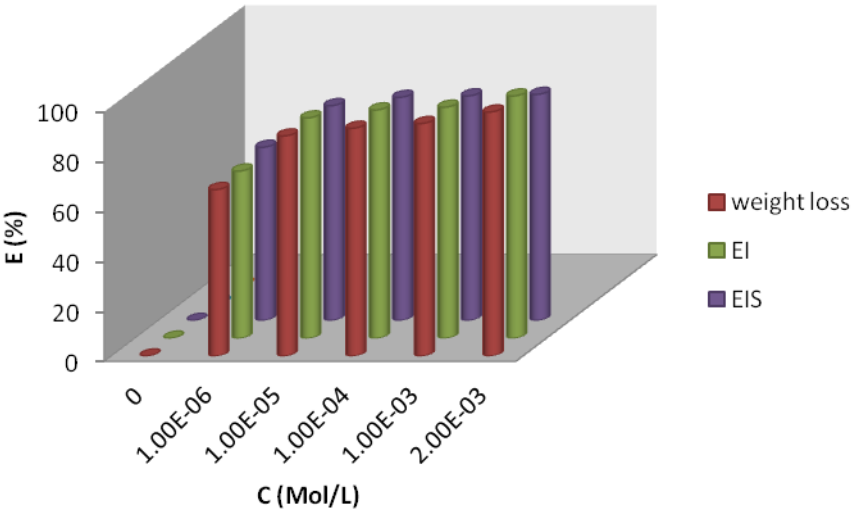

Figure 9. Comparison of inhibition efficiency (E %) values obtained by weight loss, EI and EIS methods.

3.2. Effect of temperature

3.2.1. Polarization curves

Generally, the corrosion rate of steel in acidic solution increases with rising the temperature. This is due to the decrease of hydrogen evolution overpotential [43]. For this purpose, we made potentiostatic polarization in the range of temperature 298 to 328 K, in the absence and presence of DDB at 10^{-4}M. The corresponding data are shown in fig 10, 11 and Table 4.

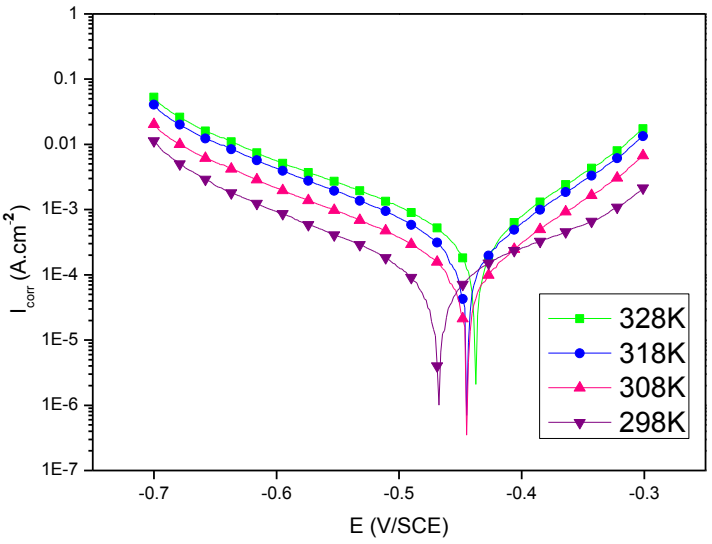

Figure 10. polarisation curves of C38 steel in 1M HCl.

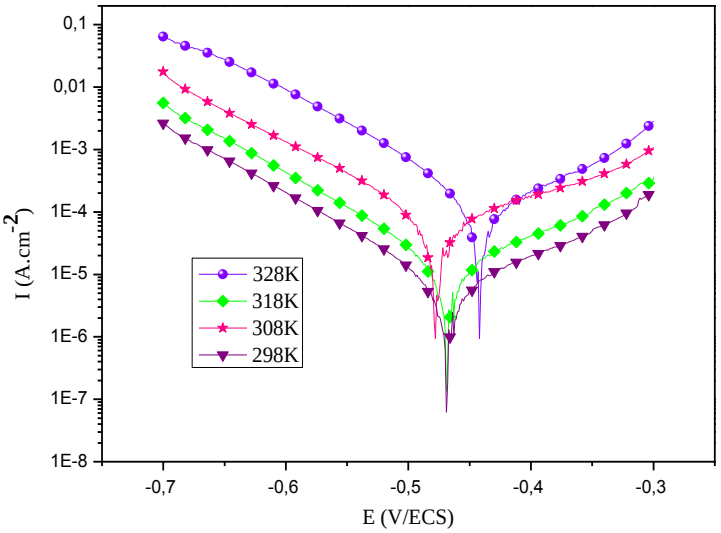

Figure 11. polarisation curves of C38 steel in 1M HCl in the presence of 10^{-4} M of DDB at different temperatures.

Table 4. Effect of temperature on the steel corrosion in the absence and presence of DDB at different concentrations.

Inhibitor	T (K)	E_{corr} (mV/SCE)	I_{corr} ($\mu A/cm^2$)	$-\beta_c$ (mV/dec)	β_a (mV/dec)	E_I (%)
Blank	298	-467	87	99	108	-
	308	-444	157	126	68	-
	318	-445	305	129	75	-
	328	-437	399	136	78	-
10^{-4} M	298	-469	8	91	91	91.5
	308	-469	15	89	81	90.4
	318	-478	84	85	84	72.5
	328	-442	231	78	83	42.1

It is clear from fig. 10 and table 4 that the increase of corrosion rate is more pronounced with the rise of temperature for blank solution. It has been observed from fig. 11 and table 4 that in the presence of DDB, I_{corr} is highly reduced. Also, the inhibition efficiencies decrease slightly with increasing of temperature indicating that higher temperature dissolution of steel predominates on adsorption of DDB at the metal surface and suggest a physical adsorption mode.

2.3 Kinetic parameters

In order to obtain more details on the corrosion process, activation kinetic parameters such as activation energies in free and inhibited acid were calculated using Arrhenius equation:

$$I_{corr} = A\exp(-\frac{Ea}{RT}) \quad (7)$$

where A is Arrhenius factor, E_a is the apparent activation corrosion energy, R is the perfect gas constant and T the absolute temperature. Plotting (log I_{corr}) versus 1/T gives straight lines as revealed from Fig.12.

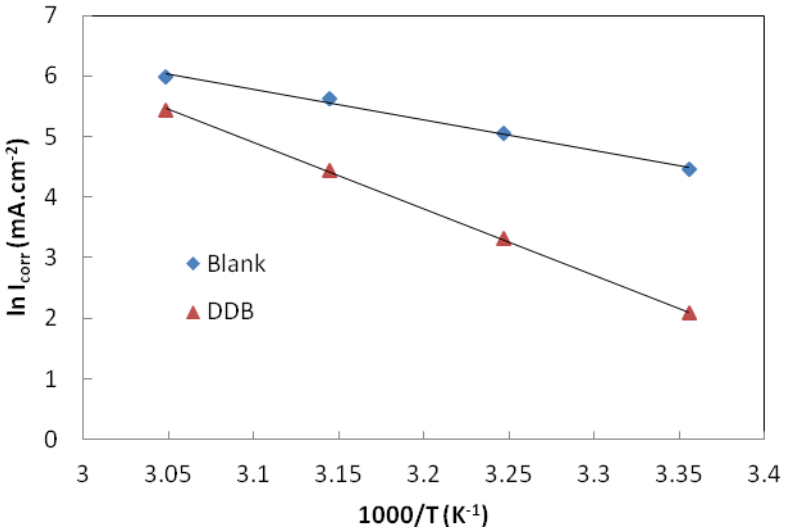

Figure 12. Arrhenius plots of steel in 1 M HCl with and without 10^{-4}M of DDB

The activation energy values obtained are 43.24 and 91.03 kJ/mol in inhibited **(**10^{-4}M of DDB) and uninhibited solutions, respectively. It is clear that the addition of inhibitor provokes an increase in the values of apparent activation energy. Popova et al. [44] pointed out that the decrease of inhibition efficiencies may be attributed to the specific interaction between the iron surface and the inhibitor components. The higher value of activation energy of the corrosion process, in the presence of DDB, is attributed to an electrostatic adsorption mechanism of the inhibitor [44-46].

Kinetic parameters, such as enthalpy and entropy of corrosion process, may be evaluated from the effect of temperature. An alternative formulation of Arrhenius equation is (6) [47]:

$$I_{corr} = \frac{RT}{Nh}.\exp(\frac{\Delta S^*}{R}).\exp(-\frac{\Delta H^*}{RT}) \quad (8)$$

Where N is the Avogadro's number, h the Plank's constant, R is the perfect gas constant, ΔS* and ΔH*the entropy and enthalpy of activation, respectively.

Fig. 13 shows a plot of ln(W/T) against 1/T for DDB. Straight lines are obtained with a slope of (-ΔH*/R) and an intercept of (ln R/Nh + ΔS*/R) from which the values of ΔH*and ΔS* are calculated respectively (Table 5).

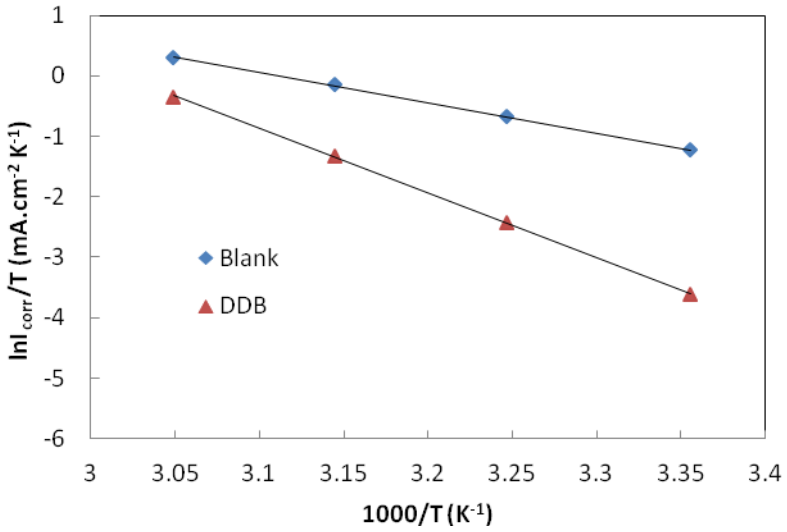

Figure13. Relation between $\ln(W_{corr}/T)$ and 1000/T in acid at different temperatures

The value of free energy ΔG* is deduced from the formula (7):

$$\Delta G^* = \Delta H^* - T\Delta S^* \quad (9)$$

Table 5. The values of activation parameters ΔH*, ΔS*and ΔG* for mild steel in 1M HCl in the absence and the presence of 10^{-4}M of DDB.

Inhibitor	Ea (kJ/mol)	ΔH* (kJ/mole)	ΔS* (J/mole^{-1}.k^{-1})	ΔG* (kJ/mole à T=298K)	Ea-ΔH*
Blank	43.24	41.57	- 181.88	95.77	2.51
10^{-4} M	91.03	88.53	- 165.29	137.78	2.50

- The ΔG* value for inhibited systems were more positive than that for the uninhibited systems revealing that in presence of inhibitor, the activated corrosion complex becomes less stable as compared to its absence.

- The positive signs of ΔH* reflecting the endothermic nature of the steel dissolution process. It is obviously that the activation energy strongly increases in the presence of the inhibitor. Some authors [48-50] have attributed this result to the inhibitor species being physically adsorbed on the metal surface.

- The increase of entropie ΔS* in the presence of inhibitor imply the corrosion system passes from a more orderly to a random arrangements with increasing the inhibitory character of the studied compound.

Similar results was recorded for some cyclic amine [51] and thiol [52] compounds when they were studied as effective corrosion inhibitors for mild steel in HCl and H_2SO_4 solutions, respectively. However, mild steel corrosion in the free acid was characterized by the more negative ΔS* value

which implies that the activation complex in the rate determining step required association rather than dissociation [53].

3.3. Adsorption isotherm

Additional information about the properties of the tested compound may be provided from the kind of adsorption isotherm. Several adsorption isotherms were tested and the Langmuir adsorption isotherm was found to provide best description of the adsorption behaviour of the investigated inhibitor. The Langmuir isotherm is given by the equation [54]:

$$\frac{C}{\theta} = \frac{1}{K} + C \qquad (10)$$

$$K = \frac{1}{55.5}\exp\left(-\frac{\Delta G_{ads}}{RT}\right) \qquad (11)$$

Where C is the inhibitor concentration, θ the fraction of the surface covered determined by E/100, k the equilibrium constant, ΔG_{ads} is the standard free energy of adsorption reaction, R is the universal gas constant, T is the thermodynamic temperature and the value of 55.5 is the concentration of water in the solution in mol/L.

Fig. 14 shows the dependence of the ratio C/ θ as function of C.

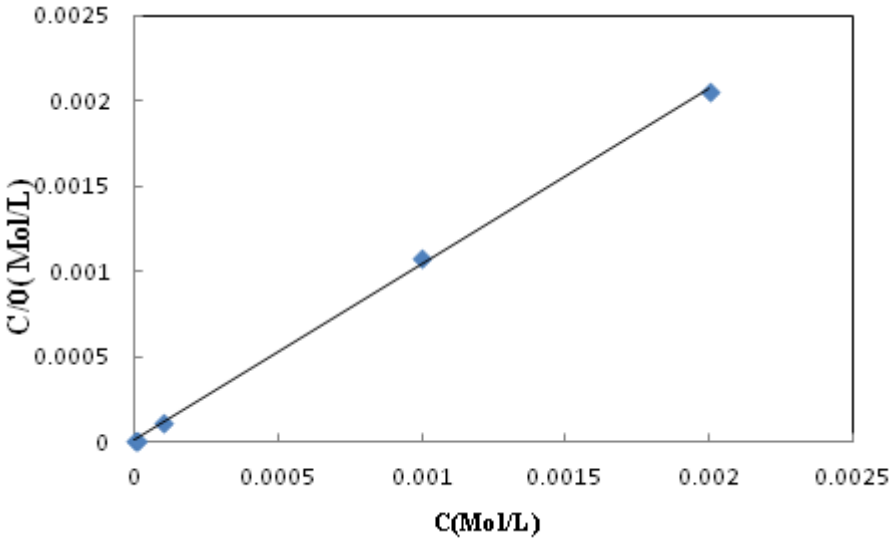

Figure 14. Plots of Langmuir adsorption isotherm of DDB at 10^{-4}M on the steel surface at 298K.

The value of ΔG_{ads} = -38.72 kJ $mol^{-1}$is too negative indicating that DDB is strongly adsorbed on the steel surface [55, 56] and ensuring the spontaneity of the adsorption process. The inhibitory action may be attributed to the presence of B, N and O atoms in the linear chain which humbly reinforces the adsorption of DDB ring.

4. CONCLUSION

The results obtained from the three different methods: potentiodynamic polarisation, EIS and weight loss, are in good agreements. and are given as follows:

* The inhibition efficiency of DDB increases with the increase of inhibition concentration to reach 97.8% at 2.10^{-3}M.

* DDB act as mixed type inhibitor without modifying the mechanism of hydrogen evolution.

*Data obtained from EIS studies were analyzed to determinate the model inhibition process through appropriate equivalent circuit models.

* The inhibition efficiency of DDB decreases with the rise of temperature.

* DDB is adsorbed on the steel surface according to the Langmuir adsorption isotherm. Thermodynamic parameters are determined.

References

1. M.A. Amin, S.S. Abd El Rehim, H.T.M. Abdel-Fatah, *Corros. Sci*. 51 (2009) 882.
2. M. Ozcan, F. Karadag˘, I. Dehri, *Colloid Surface A*. 316 (2008) 55.
3. E.E. Oguzie, Y. Li, F.H. Wang, *Electrochim. Acta*. 53 (2007) 909.
4. E.E. Oguzie, Y. Li, F.H. Wang, *J. Colloid & Interf. Sci*. 310 (2007) 90.
5. A.B. Silva, S.M.L. Agostinho, O.E. Barcia, G.G.O. Cordeiro, E. D'Elia, *Corros. Sci*. 48 (2006) 3668.
6. O. Olivares, N.V. Likhanova, B. Gomez, J. Navarrete, M.E. Llanos-Serrano, E Arce, J.M. Hallen, *Appl. Surf. Sci.* 252 (2006) 2894.
7. S. Aezola, J. Genesca, *J. Solid State Electrochem*. 8 (2005) 197.
8. H. Zarrok, H. Oudda, A. Zarrouk, R. Salghi, B. Hammouti, M. Bouachrine, *Der Pharma Chemica.* 3 (2011) 576.
9. M. Zerfaoui, B. Hammouti, H. Oudda, M. Benkaddour, *Prop. Org. Coat.* 51 (2004) 135.
10. K. Bouhrira, F. Ouahiba, D. Zerouali, B. Hammouti, M. Zertoubi, N. Benchat, *J .Chemistry.* 7 (2010) S35.
11. S.A. Abd El Maksoud, *J. Electroanal. Chem.* 565 (2004) 321.
12. Y. Abboud, B. Ihssane, B. Hammouti, A. Abourriche, S. Maoufoud, T. Saffaj, M. Berrada, M. Charrouf, A. Bennamara, H. Hannache, *Desal & Water Treat*, 20 (2010) 35. 1202.
13. M. Zerfaoui, H. Oudda, B. Hammouti, M. Benkaddour, S. kertit, M. Zertoubi, M. Azzi, M. Taleb, *Revue de Metall*. 99 (2002) 1105.
14. A. Yahyi, A. Aouniti, B. Hammouti, A. Ramdani, S. Kertit, *Trans. SAEST*. 39 (2004) 5.
15. A. Anejjar, R. Salghi, A. Zarrouk, O. Benali, H. Zarrok, B. Hammouti, E. E. Ebenso. *J. Assoc. Arab. Univer Bas & Appl Sci*., 15 (2014) 21.
16. R. Salghi, B. Hammouti, A. Aouniti, M. Berrabah, S. Kertit, *J. Electrochem. Soc. India*. 49 (2000) 40.
17. B. Zerga, A. Attayibat, M. Sfaira, M. Taleb, B. Hammouti, M. Ebn Touhami, S. Radi, Z. Rais, *J. Appl. Electrochem.* 40 (2010) 1575.
18. K. Tebbji, A. Aouniti, A. Attayibat, B. Hammouti, H. Oudda, M. Benkaddour, S. Radi, A. Nahle, *Ind J. Chem. Techn.* 18 (2011) 244.
19. L. Herrag, B. Hammouti, S. Elkadiri, A. Aouniti, C. Jama, H. Vezin, F. Bentiss, *Corros. Sci.* 52 (2010) 3042.
20. M. Benabdellah, A. Yahyi, A. Dafali, A. Aouniti, B. Hammouti, A. Bnettouhami. *Arab. J. Chem.* 4 (2011) 343
21. H. Ashassi-Sorkhabi, Z. Ghasemi, D. Seifzadeh, *Appl. Surf. Sci.* 249 (2005) 408.

22. M. Bouklah, A. Attayibat, B. Hammouti, A. Ramdani, S. Radi, M. Benkaddour, *Appl. Surf. Sci*. 240 (2005) 341.
23. A. El-Ouafi, B. Hammouti, H. Oudda, S. Kertit, R. Touzani, A. Ramdani, *Anti-Corros. Met. Mater*. 49 (2002) 199.
24. N. Huynh, S.E. Bottle, T. Notoya, A. Trueman, B. Hinton, D.P. Schweinsberg, *Corros. Sci*. 44 (2002) 1257.
25. R. Salghi, L. Bazzi, B. Hammouti, E. Zine, S. Kertit, S. El Issami, E. Ait Eddi, *Bull. Electrochem*. 17 (2001) 429.
26. A. Chetouani, K. Medjahed, K.E. Sid-Lakhdar, B. Hammouti, M. Benkaddour, A. Mansri, *Corros. Sci*. 46 (2004) 2421.
27. A.Ousslim, A. Aouniti, K. Bekkouch, A. Elidrissi, B. Hammouti, S. *Review & Letters*. 16 (2009) 609.
28. K. Tebbji, H. Oudda, B. Hammouti, M. Benkaddour and S. S. Al-Deyab, A. Aouniti, S. Radi, A. Ramdani, *R. Chem. Intermed*. 37 (2011) 985.
29. M. Elayyachy, B. Hammouti, A. El Idrissi, A. Aouniti, *Port. Electrochim. Acta*. 29 (2011) 57.
30. M.T. Saeed, *Anti-Corros. Met. Mater*. 51 (2004) 389.
31. L.G. Qiu, A.J. Xie, Y.H. Shen, *Corros. Sci*. 47 (2005) 273.
32. S. Muralidharan, M.A. Quaraishi, S.V.K. Iyer, *Corros. Sci.* 37 (1995) 1739.
33. S. Kertit, B. Hammouti, *Appl. Surf. Sci.* 93 (1996) 59.
34. A .Y .El-Etre, *Materials Chem & Phys.* 108 (2008) 278.
35. H. Shih, H. Mansfeld, *Corros. Sci*. 29 (1989) 1235.
36. WB. Wan Nik, O. Sulaiman, A.F. Ayob, M.F. Ahmad, M.M. Rahman, *Int. J. Eng. Res & App.*, 2 (2012) 455.
    M. Benabdellah, A. Yahyi, A. Dafali, A. Aouniti, B. Hammouti, A. Ettouhami, *Arabian. J. Chem*. 4 (2011) 243
37. J.R. Macdonald Impedance, A. Wiley, *Intersci. Publ*, (1987).
38. J.R. Macdonald, *J. Electroanal. Chem*, 25 (1987) 223.
39. S.F. Mertens, C. Xhoffer, B.C. De Cooman, E. Temmerman, *Corros.* 53 (1997) 381
40. E. McCafferty, *Corros. Sci.* 39 (1997) 243.
41. M.S. Morad, *Corros. Sci*. 42 (2000) 1313.
42. F. Bentiss, M. Lagrenée, M. Traisenl, J. C. Hornez, *Corros. Sci*. 41(1999) 789
43. M.S. Morad, *Corros. Sci*. 42, 1313 (2000).
44. A. Popova, E. Sokolova, S. Raicheva, M. Christov, Corros. Sci. 45 (2003) 33.
45. H. Zarrok, A. Zarrouk, R. Salghi , B. Hammouti, N. Chahboun, D. Ben Hmamou, R. Hmammouchi, T. Lakhlifi, A. Rochdi , A. El Assyry, *Mor. J. Chem*. 2 (1) (2014) 10.
46. F. Mounir, S. El Issam1, Lh. Bazzi, O. Jbara, A. Chihab Eddine, M. Belkhaouda, L. Bammou, R. Salghi, L. Bazzi, *Mor. J. Chem*. 2(1) (2014) 33.
47. S.S. Abd-El-Rehim, S.A.M. Refaey, F. Taha, M.B. Saleh, R.A. Ahmed, *J. Appl. Electrochem*. 31 (2001) 429.
48. Z. Faska, A. Bellioua, M. Bouklah, L. Majidi, R. Fihi, A. Bouyanzer, B. Hammouti, *Monatshefte für Chemie*. 139 (2008) 1417.
49. A. Bouyanzer, B. Hammouti, *Pigm. Resin & Techn*. 33 (2004) 287.
50. Y. Abboud, A. Abourriche, T. Ainane, M. Charrouf, A. Bennamara, O.Tanane, B Hammouti, *Chem. Eng. Comm.* 196 (2009) 788.
51. A. El Awady, A. Abd El Naby, S. Aziz, *J. Electrochem. Soc*. 139 (1992) 2149.
52. M.Th. Makhlouf, M.H. Wahdan, *Pol. J. Chem.* 69 (1995) 1072.
53. S.S. Abd-El-Rehim, S.A.M. Refaey, F. Taha, M.B. Saleh, R.A. Ahmed, *J. Appl. Electrochem.* 31(2001) 429.
54. F. Mansfeld, M.W. Kending, S. Tsai, *Corros*. 37 (1982) 301.
55. J.D. Talati, D.K. Gandhi, *Corros. Sci*. 23 (1983) 1315.

56. G.K. Gomma, M.H. Wahadan, *Indian J. Chem. Technol*. 2 (1995) 107.